

A prototype transformer for inductive contactless energy transfer system: numerical models verified by measurement

Abstract. This paper describes results of simulation of a transformer used in a prototype of energy supply system. The finite element models with use of Argos2D and COMSOL Multiphysics software were constructed to predict lumped parameter model of the power supply system. Computer simulation provides an easy way of estimation of the basic transformer parameters, some of which can be hard to measure in reality, but obtained values should be verified by measurements. The authors compare different methods and models used for lumped parameters calculation and discuss their accuracy.

Streszczenie. W artykule przedstawiono wyniki symulacji prototypowego transformatora do bezkontaktowego transferu energii. Celem było wyznaczenie parametrów zastępczego modelu obwodowego. Porównano wyniki otrzymane przy wykorzystaniu 2- i 3-wymiarowych modeli transformatora zestawione z wynikami pomiarów. Oszacowano też dokładność otrzymanych wartości. Porównanie wyników symulacji komputerowych i pomiarów parametrów obwodowych transformatora do bezkontaktowego przekazywania energii

Keywords: transformer, numerical field simulation, lumped parameters

Słowa kluczowe: transformator, komputerowa symulacja rozkładu pola, zastępcze parametry obwodowe

doi:10.12915/pe.2014.05.11

Introduction

Personal Rapid Transit (PRT)[1, 2] is an interesting, yet not widely used type of automated guided transit system. Some of its features, like point-to-point travel ability or separate railways, are believed to be effective in solving traffic problems of emerging large metropolises. Different types of power supply are considered for use in PRT systems. The one relevant for this study is based on the contactless energy transfer (CET) by means of electromagnetic induction. The CET transformer is an integral part of the contactless energy supply system constructed by a group from the Electrical Drive Division of the Electrical Engineering Department, Warsaw University of Technology in cooperation with the Faculty of Transport as an element of the "Eco-mobility" project. In order to properly design and optimize the CET system it is necessary to perform a magnetic field simulation. Suitable transformer simulation allows for the introduction of design modifications without having to construct a physical model. In this paper we focus on transition from the field simulations to the lumped parameters of the transformer.

Fig. 1 shows a scaled vehicle with a concept model of a CET transformer where primary winding, in a form of a 1-turn loop, is distributed along the PRT guide way.

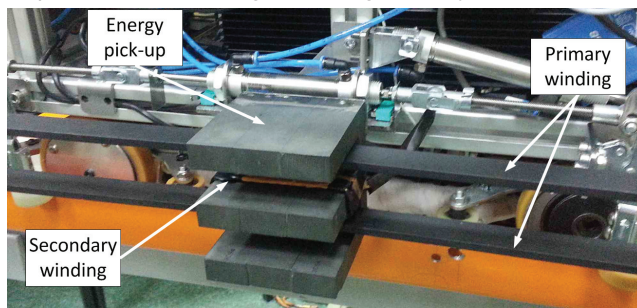


Fig. 1. The transformer prototype

The E-shaped core, with secondary winding (10 turns), mounted on the center column creates energy pick-up, which is located on the vehicle. The core of the proposed transformer consists of three equally spaced columns made of 3C90 Ferroxcube material [3], with the loop as the primary winding (of approximately length of 1 meter). The basic dimensions of the transformer are the following: thickness d – 0.084 m, height h – 0.109 m, column width cw – 0.016 m, width of the gap between the columns gw – 0.0225 m. The

linear model of the ferromagnetic material (justified with relatively small values of the magnetic flux density in the core) with $\mu_r = 1000 \div 1600$ were tested. In this range of relativity we have observed only a minor dispersion of the computed values of inductances.

The unusual design of the transformer with an open core and relatively big leakage flux raises up some difficulties with measuring the mutual and leakage inductances of the device, required in circuital description of the system. The transformer's circuit model used to design the power supply system is shown in Fig. 2. The circuital description of the whole

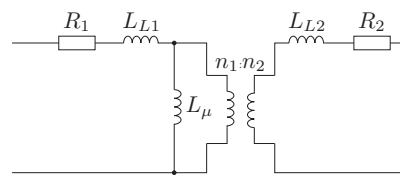


Fig. 2. The circuital model of the transformer

system plays a crucial role in design of the power supply working in the resonant mode. The goal of numerical simulations is to determine the values of equivalent leakage inductances L_{L1} and L_{L2} which are related to self- and mutual inductances of the coils:

$$(1) \quad L_{L1} = L_1 - \frac{n_1}{n_2} M,$$

$$(2) \quad L_{L2} = L_2 - \frac{n_2}{n_1} M,$$

where L_1 stands for the self inductance of the primary coil, L_2 for the self inductance of the secondary coil, $n_1 = 1$ is the number of the turns for the primary and $n_2 = 10$ for the secondary coil and M is the mutual inductance. In order to verify the values and to estimate the accuracy we have used 2D and 3D numerical models and various methods of calculation of inductances. Finally the obtained values were compared with the results of the measurements.

The models

Two-dimensional models of transformer were created independently in two programs: COMSOL Multiphysics (commercial) and Agros2D (open source). After the initial evaluation we noticed that the open source tool, implementing the higher order elements and hp-adaptivity offers much higher

precision in 2D. Due to inability to model the changes of magnetic flux density along the axis parallel to d dimension of transformer the 2D model consists of two parts: the more complicated, simulating the cross-section of the pick-up core and coil and the simpler one, modelling only the leakage flux of the primary winding far from the pick-up device. The model of pick-up, more crucial for computations, is shown in Fig. 3.

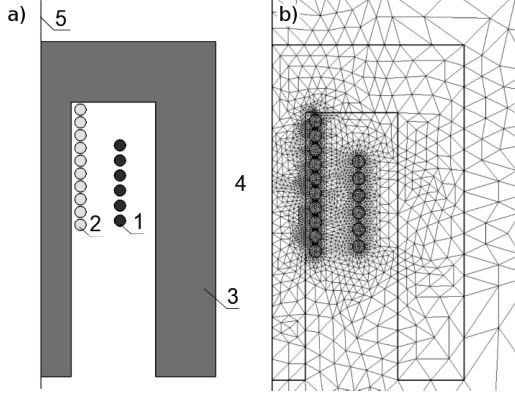


Fig. 3. a) Geometry of the 2D-transformer model, created in Agros2D: 1 – the primary winding 2 – the secondary winding, 3 – the core of the transformer, 4 – air surrounding the transformer, 5 – the symmetry plane, b) the refined finite element mesh of the Agros2D model

The 3D model of the transformer was created in COMSOL Multiphysics. For the sake of effectiveness and precision, we exploited the symmetries modelling only the 1/4 of the transformer. The model geometry is shown in Fig. 4.

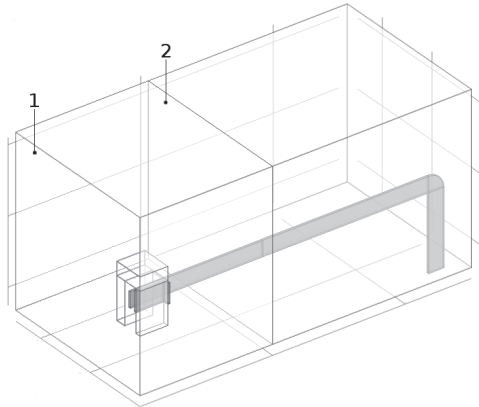


Fig. 4. The 3D transformer model: the whole finite element domain, with the respective 2D models planes shown, 1 – cross-section of the pick-up core, 2 – cross-section of the leakage zone

The methods of calculation

It is well known that the self inductance of a coil, L , is well defined in case of the electrical circuit, where it can be taken as a ratio between the voltage drop on the lumped element (a coil) – u and time derivative of the element's current i :

$$(3) \quad u_1 = L \frac{di_1}{dt}.$$

The mutual inductance M is defined in the same way but it relates the voltage excited in one coil with the time derivative of another coil's current:

$$(4) \quad u_1 = M_{12} \frac{di_2}{dt}.$$

The idea of inductance is based on storage of the energy in the magnetic field produced by the coil but the distributed

(EM field theory) definition usually relates the coil's current I and the self-coupled magnetic flux produced by the coil Ψ :

$$(5) \quad L = \frac{\Psi}{I}.$$

This definition is usually presented for an idealized, single-turn coil made of infinitely thin wire, where the flux or the coupled flux can be precisely defined as the surface integral of magnetic flux density B or the circulation of magnetic vector potential A :

$$(6) \quad L = \frac{\int_S \mathbf{B} \cdot d\mathbf{S}}{I} \quad \text{or}$$

$$(7) \quad L = \frac{\oint_{\partial S} \mathbf{A} \cdot d\mathbf{l}}{I}.$$

where S is the surface being bounded by ∂S —the current line and the magnetic vector potential A is defined by the well known formula $\nabla \times \mathbf{A} = \mathbf{B}$. The later form (circulation of A) is usually easier to compute in numerical field simulation software.

The mutual inductance can be computed as the relation of the magnetic flux produced by the primary winding passing through the secondary winding and the current causing the flux:

$$(8) \quad M_{12} = \frac{\Psi_{12}}{I_1} = \frac{\int_{S_2} \mathbf{B}_1 \cdot d\mathbf{S}_2}{I_1} = \frac{\oint_{\partial S_2} \mathbf{A}_1 \cdot d\mathbf{l}_2}{I_1}.$$

In (8) the indices refer to the first (producer) and the second (receiver) coils respectively: we need to integrate the magnetic flux density or vector potential excited by the “first” coil across the surface or along the path of the current in the “second” coil. It is well known, that by exchanging the indices in (8) we should get the same value of the mutual inductance.

In circuital models the mutual inductance is often defined with help of the coupling coefficient k which describes the average ratio of flux produced by one coil coupled with the other one. Knowing k one can calculate the mutual inductance of two coils as

$$(9) \quad M_{12} = k \sqrt{L_1 L_2}.$$

Computation of $k = \sqrt{k_1 k_2}$ in numerical models is similar to computation of coupled flux: $k_1 = \Psi_{12}/\Psi_1$, $k_2 = \Psi_{21}/\Psi_2$.

The most important difficulty in practical application of the above formulas is that the meaning of “flux” for a coil consisting of a few turns which are made of a real wire is not precise. It's worth noticing, that the path of integration (∂S) in (7) is in such case neither precise, nor closed for the majority of numerical coil models, where the wire model is not a closed, infinitely thin line. The same problem affects equation (6), for which the surface S is hard to be precisely identified in the numerical model.

This problem can be generally solved with the use of very general Neumann's formula for the mutual inductance of two predefined current density distributions:

$$(10) \quad M_{i,j} = \frac{\mu}{4\pi} \frac{1}{I_i I_j} \int_{V_i} \int_{V_j} \frac{\mathbf{J}_i(\vec{r}_i)}{\mathbf{J}_j(\vec{r}_j)} |\vec{r}_i - \vec{r}_j| dV_i dV_j,$$

but this equation needs to be implemented in the finite element program or eventually written as a specialized postprocessor if the simulation program allows exporting the distribution of the current density vector J .

The authors of [6] have proposed a method in which the line integration in (7) is replaced with the integration over the

volume of the coil. According to this method the coupled flux can be calculated as

$$(11) \quad \Psi = \frac{N}{S_{coilX}} \int_{V_{coil}} \mathbf{A} \cdot \mathbf{1}_J dV,$$

where N is the number of turns, V_{coil} – the volume of coil, $\mathbf{1}_J$ – the unit vector parallel to the local direction of the current density vector \mathbf{J} and S_{coilX} is the coil cross-section. Originally the formula is split into a sum of integrals over the finite elements forming the coil but this complication is necessary only if the cross-section of the coil is not constant along the current flow.

The more precise and usually much more convenient formula for self inductance can be derived from the well known equation for the energy stored in the magnetic field of a coil [4]:

$$(12) \quad L = \frac{2W}{I^2},$$

where W is the magnetic energy and I is the current in the coil. The magnetic energy W can be calculated by integration of the magnetic field energy density over the volume of the whole model with only a single coil fed with the current I . For the linear model of the core we get:

$$(13) \quad W = \int_V \frac{\mathbf{H} \cdot \mathbf{B}}{2} dV.$$

The magnetic flux density \mathbf{B} and magnetic field intensity \mathbf{H} can be easily calculated at any point of the model. Moreover, if the finite element method is used for simulation, the total energy in the whole model domain is computed with the much higher precision than the local values of the potential or derived field quantities [7, 4].

The formula (12) is valid only for idealized, linear models of the ferromagnetic material and can not be used for mutual inductance calculation. Thus, in general the use of the formula (11) seems to be the best computational method.

Self inductances of primary and secondary windings

Throughout this paper we assume the active circuit is fed with unit current (1A), which greatly simplifies computations.

To calculate the self inductance of the primary coil we feed it with the current and calculate the coupled flux (as in (5) or (11)) or the total energy stored in the model domain (as in (12)). The latter formula is easy for application: most of packages for numerical field simulation offers integration of the total energy stored in the system out of box, without any special effort of the user. The only difficulty is in the 2D model where we need to simulate separately the core section and the primary winding alone (compare with Fig. 4).

The constant lines of the magnetic vector potential \mathbf{A} in the 2D models are shown in Fig. 5. The left inset presents the results for the pick-up section and the right inset shows the field of the primary winding far from the pick-up device.

Total energy stored in the system was $2.882 \mu\text{J}$ per 1 meter of length for the pick-up section and $0.3988 \mu\text{J/m}$ in the "leakage" section. Multiplying these values by the lengths of the respective sections we get the total energy of $2.882 \cdot 0.084 + 0.3988 \cdot 0.816 = 0.5675 \mu\text{J}$ and the self inductance of the primary winding calculated with (12) is $L_1 = 1.135 \mu\text{H}$. To calculate the self inductance by (5) we need to estimate the self-coupled flux, what can be done on the basis of the magnetic vector potential \mathbf{A} distribution (see Fig. 5) or on the basis of the values of the magnetic flux density \mathbf{B} (see (6),(7)). The latter is computed by numerical derivation of \mathbf{A} , so the result obtained with \mathbf{A} should be more

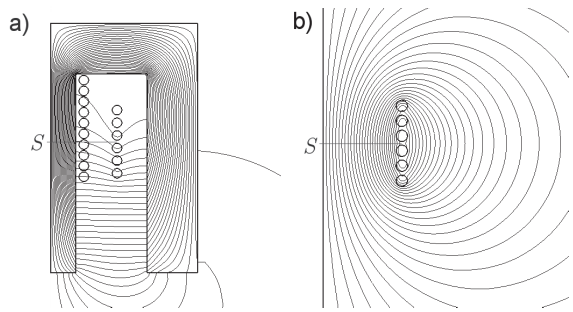


Fig. 5. Magnetic vector potential excited by the primary coil in Agros2D model of the transformer: a) pick-up section, b) leakage field far from the pick-up

exact, and this one obtained with \mathbf{B} can be used to estimate of the inaccuracy in value of L .

The plot of \mathbf{A} in the left inset of Fig. 5 shows 30 equilines drawn every 102.7 nWb (per 1 meter of the model length). As we can calculate (by a simple summation of the inter-line partial fluxes) the total flux produced by the primary coil is equal to $2.9783 \mu\text{Wb/m}$ and $24/29$ of it is coupled with the total current of the same coil. Next $2/29$ of the flux is coupled with $5/6$ of the current, another $2/29$ with $1/2$ of the current, and yet one $1/29$ with $2/6$ of the current (as you can see in Fig. 5 the coil cross-section was logically divided into six sections to simplify this estimation). The total coupled flux in the "leakage zone" can be thus estimated as $102.7 \cdot (1 \cdot 24 + 5/6 \cdot 2 + 1/2 \cdot 2 + 2/6 \cdot 1) = 2772.9 \text{ nWb/m}$.

The plot in the right inset of Fig. 5 shows 30 equilines drawn every 14.63 nWb/m thus the total flux produced by the primary coil in air is equal to 424.27 nWb/m and approximately $23/29$ of it is coupled with the total current. Next $4/29$ of the flux is coupled with $2/3$ of the current and next $2/29$ with $1/3$ of the current. The total coupled flux in the "leakage" section can be thus estimated as $14.63 \cdot (1 \cdot 23 + 2/3 \cdot 4 + 1/3 \cdot 2) = 385.257 \text{ nWb/m}$.

The partial fluxes were computed in the model constituting the half of the device, thus the self inductance of the primary coil calculated with (5) can finally be estimated as $L_1 = 2 \cdot (2772.9 \cdot 0.084 + 385.257 \cdot 0.816)/1 = 1.0946 \mu\text{H}$.

The coupled flux can also be estimated from the 2D model by the integration of the magnetic flux density in the cross-section of the coil. Using the integration lines marked as S on Fig. 5 we have obtained $2.948 \mu\text{Wb/m}$ in the pick-up and $0.43 \mu\text{Wb/m}$ in the "leakage" section. Merging both results we have obtained $L_1 = 2 \cdot (2.948 \cdot 0.084 + 0.43 \cdot 0.816)/1 = 1.197 \mu\text{H}$.

Application of (11) is theoretically possible for 2D finite element codes, but not supported by Agros2D and thus was not performed.

Summarizing: calculation of L_1 with 2D field model and three different methods gave us three slightly (within 10% of the smallest value) different results. These differences will be discussed in details in the concluding section.

The 3D model of transformer built with COMSOL Multiphysics allows us to simulate the non-uniform distribution of the magnetic field at the ends of the pick-up device. The comparison of the magnitude of \mathbf{B} in the central column of the core simulated with the 2D and the 3D models (Fig. 6) shows clearly the advantage of the 3D model. We can observe an effect of the reinforcement of \mathbf{B} in the core of the 3D compared to the 2D model. This obviously will result in a bigger value of the flux and also the bigger inductance of the coil.

The self inductance of the primary coil can easily be calculated with the 3D model and (12). COMSOL Multiphysics

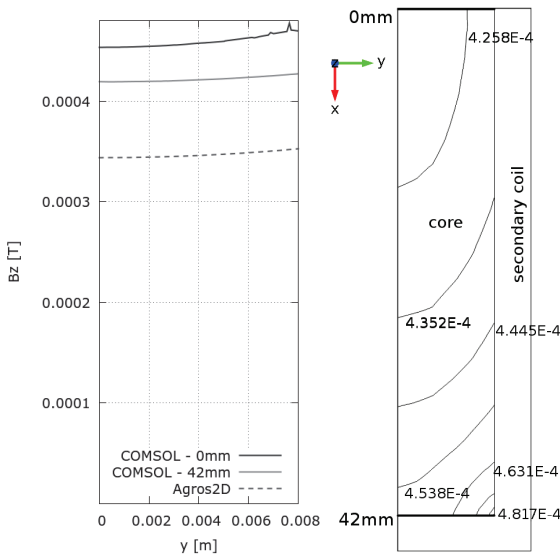


Fig. 6. Magnetic flux density in the central column of the pick-up core: a) the comparison of B_z in the 2D model and in the 3D model, b) the isolines of B_z in the core cross-section of the 3D model

supports the volume integration of practically any expression involving field quantities. Using the model presented in Fig. 4 it is then straightforward to obtain the value of the total energy stored in the magnetic field – $0.17575 \mu\text{J}$, what multiplied by 4 (we have simulated only 1/4 of the device) gave us $L_1 = 1.406 \mu\text{H}$. As expected, this value of inductance is larger than that obtained in the 2D model.

Calculation of the coupled flux by integration of the magnetic vector potential \mathbf{A} along the chosen contour is not very well supported in COMSOL. To do this one needs to add several artificial cross-sections of the model geometry and, moreover, the program can only integrate cartesian components (and not the tangential to the path of integration). For this reason, the integration of \mathbf{B} , which is much better supported in COMSOL, was performed. Integration of the flux density crossing the lower surface of primary winding gave us $\Psi_1 = 0.348 \mu\text{Wb}$, what multiplied by 4 and divided by the total current gave $L_1 = 1.392 \mu\text{H}$.

Application of (11) is well supported in COMSOL. In our case integration of the A_x (see Fig. 4) over the long part of the coil and $-A_z$ over the short part, substituted into (11) reads: $\Psi_1 = (1.3294e - 12 - 2.56358e - 11)/6.9e - 5 = -3.523e - 6$ what gives $L_1 = 4 \cdot |\Psi_1|/1 = 1.409 \mu\text{H}$.

The self inductance of the secondary (pick-up) coil was also calculated with the all presented methods. The results are summarized in Table 1.

Table 1. Self inductances of the primary and secondary coils computed with different methods

Method (equation)	2D			3D		
	(12)	(7)	(6)	(12)	(6)	(11)
$L_1 [\mu\text{H}]$	1.135	1.0946	1.197	1.406	1.392	1.409
$L_2 [\mu\text{H}]$	62.20	58.30	60.35	67.88	68.63	68.04

The mutual inductance

The mutual inductance M_{12} was computed using both methods expressed in (8), that of (9) using the coupling coefficient k calculated with the help of the 2D model and with help of (11) for the 3D model.

It is obvious that while the mutual inductance can be calculated by feeding the primary winding and assessing flux coupled with the secondary winding or by feeding the secondary winding and assessing flux coupled with the primary

winding, both methods should give similar results.

In 2D, if the primary coil is fed, we need to consider two variants of the model as shown in Fig. 5. Analysing the field shown in the left inset we can see (using the same method as for the self-inductance, but this time counting lines coupled with the secondary winding) that 23/29 of the total flux produced by the primary coil ($2.9783 \mu\text{Wb/m}$) is coupled with the whole secondary winding, next 1/29 with 9 turns, next 2 with 8 turns, 1/29 with 7 turns, 1/29 with 6 and 1/29 of the flux with 3 turns only. Thus we can estimate the coupling coefficient in the pick-up zone: $k_{1p} = 23/29 + 0.9 \cdot 1/29 + 0.8 \cdot 2/29 + 0.7 \cdot 1/29 + 0.6 \cdot 1/29 + 0.3 \cdot 1/29 = 0.9345$.

In the “leakage” zone a zero portion of the flux produced by the primary winding is coupled with the secondary one. Thus, to calculate the total coupling coefficient we must weight k_{1p} by the ratio of the flux in the pick-up zone to the total flux produced by the primary winding. Using the values already presented in the previous section we get:

$$k_1 = k_{1p} \cdot \frac{2.9783 \cdot 0.084}{2.9783 \cdot 0.084 + 0.42427 \cdot 0.816} = 0.392$$

If the secondary coil is fed we can restrict the 2D model to the pick-up zone and calculation of k_2 based on the field plot presented on Fig. 7. Then $k_2 = 22/29 + 5/6 \cdot 1/29 + 4/6 \cdot 2/29 + 3/6 \cdot 1/29 + 2/6 \cdot 1/29 = 0.862$. The final

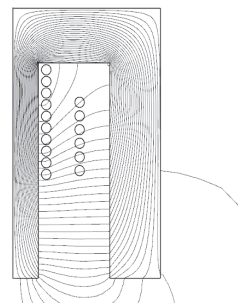


Fig. 7. Magnetic vector potential excited by the secondary coil in the Agros2D model of the transformer's pick-up section
value of the coupling coefficient calculated with the 2D model is then $k = \sqrt{0.392 \cdot 0.862} = 0.581$

Using (9) and values of L_1, L_2 from Table 1 (for 2D only) we obtain $4.641 \leq M_{12} \leq 5.013 \mu\text{H}$.

To compute M_{12} using (8) we have to estimate the flux coupled with the secondary winding. It can be done on the basis of magnetic vector potential \mathbf{A} distribution. Using the same method as in the case of self-inductance computations one can see that the coupled flux can be computed as: $102.7 \cdot (23 + 0.9 \cdot 1 + 0.8 \cdot 2 + 0.7 \cdot 1 + 0.6 \cdot 1 + 0.3 \cdot 1) = 2783.17 \text{ nWb/m} = 2.7832 \mu\text{Wb/m}$. Multiplying the flux by the length of the pick-up zone (0.084 m) we shall get the mutual inductance: $M_{12} = (2 \cdot 10 \cdot 2.7832 \cdot 0.084)/1 = 4.6758 \mu\text{H}$, where the factor of 2 comes from the fact that only half of the device was modelled and factor of 10 is the number of turns in secondary winding.

Magnetic flux produced by the secondary winding passing through the primary winding, can be estimated with field plot presented in Fig. 7 by addition of partial fluxes (each of $1.141 \mu\text{Wb/m}$), coupled with the primary winding. 22 of 29 flux isolines on Fig. 7 are fully coupled with the primary winding, next one with 5/6, next 2 with 4/6, one with 3/6 and the last one with 2/6 of the winding. The coupled flux can be estimated as: $1.141 \cdot (22 + 5/6 \cdot 1 + 4/6 \cdot 2 + 3/6 \cdot 1 + 2/6 \cdot 1) = 28.525 \mu\text{Wb/m}$. Then the value of mutual inductance is computed as $M_{21} = 2 \cdot 0.084 \cdot 28.525 = 4.7922 \mu\text{H}$.

In the case of the 3D model we can estimate the flux produced by the primary and coupled with the secondary coil

on the base of the surface integrals. For example we can use surfaces S_b – at the bottom of the secondary winding, S_m in the middle of it and S_t at the top of the winding (as it is shown in Fig. 8). The whole flux calculated on S_b couples with the secondary winding, and those computed on S_m and S_t are only partially coupled. We could try to estimate the coupling coefficients on the base of the 2D model, but as shown in the previous section the field distributions are different in 2D and 3D and such estimation would be inaccurate. Thus we have decided to take the middle integral as the simplest estimate. This choice was justified during calculation of self inductances in the 3D model. Several trials showed that using the flux through the plane in the middle of the coil gives the closest value to those obtained with the total energy of magnetic field. For this reason we have decided to apply the same strategy here.

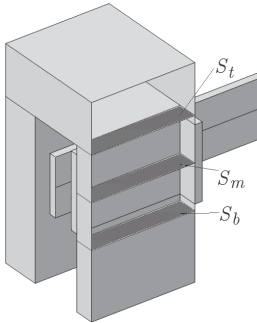


Fig. 8. Planes used to estimate the flux coupled to the secondary coil $\Phi_{S_t} = 0.1587 \mu\text{Wb}$, $\Phi_{S_m} = 0.1465 \mu\text{Wb}$, $\Phi_{S_b} = 0.1246 \mu\text{Wb}$

Feeding the primary winding we have obtained the total flux produced $\Phi_1 = 0.31499 \mu\text{Wb}$; $\Phi_{12} = 0.1465 \mu\text{Wb}$ was coupled with the 10-turn secondary coil giving $M_{12} = 4 \cdot 10 \cdot 0.1456/1 = 5.858 \mu\text{H}$. The coupling coefficient can be estimated as $k_1 = 0.1465/0.31499 = 0.46$. This value is much bigger than k_1 obtained on the basis of the 2D model.

Feeding the secondary winding we have got the total flux $\Phi_2 = 1.7157 \mu\text{Wb}$; $\Phi_{21} = 1.5064 \mu\text{Wb}$ and $M_{21} = 4 \cdot 1.5064/1 = 6.0256 \mu\text{H}$. The coupling coefficient can be estimated as $k_2 = 1.5064/1.7157 = 0.8779$.

Calculating the coupled fluxes with (11), feeding the primary coil and calculating the integral over the secondary one we got the coupled flux in the model equal to $\Phi_{12} = 0.1475 \mu\text{Wb}$ and the mutual inductance $M_{12} = 5.9 \mu\text{H}$. Feeding the secondary coil we have got $\Phi_{21} = 1.505 \mu\text{Wb}$ and the mutual inductance $M_{21} = 6.02 \mu\text{H}$.

All computed values of the mutual inductances are summarized in Table 2.

Table 2. Mutual inductances computed with different methods

Method (equation)	2D		3D		
	(8)	(9)	(8)	(9)	(11)
$M_{12} [\mu\text{H}]$	$4.641 \div 5.013$	4.7922	$6.177 \div 6.224$	5.858	5.90
$M_{21} [\mu\text{H}]$	4.6758		6.026	6.02	

Discussion and conclusion

The inductances were measured with Hameg HM8118 LCR bridge at 50 kHz. The mutual inductance were measured with two different methods giving slightly different values of 5.55 and 5.76 μH . The first value was taken with the use of HZ186 transformer test cable adapter for HM8118. In the second method the primary and secondary windings were connected serially in two different directions (to add and to subtract the magnetic flux) and in such configurations the total inductances L_{T+} and L_{T-} were measured. Then it was easy to calculate M knowing that

$$(14) \quad L_{T+} = L_1 + L_2 + 2M, \quad L_{T-} = L_1 + L_2 - 2M.$$

According to the specification of the HM8118 the measurement accuracy can be estimated as 0.2% for the direct measurement of inductance. Error evaluation for (14) suggest that this value should be multiplied by $\sqrt{3}/2$ giving practically the same accuracy for the mutual inductance.

In Table. 3 the averaged values obtained by numerical simulation are compared with the measured parameters of a prototype. A very good agreement was obtained and the differences can be explained by uncertainty in material properties of the core. The relative permeability of 3C90 reaches value of 1500 for the operating frequency and this value was finally used in simulations. However, the actual value for the used core depends much on the assembly process and can be significantly lower, influencing the leakage flux and thus the inductances.

Table 3. Comparison of inductances: averaged values of simulation against measured values.

	$L_1 [\mu\text{H}]$	$L_2 [\mu\text{H}]$	$M [\mu\text{H}]$
2D model	1.142	60.281	4.763
3D model	1.399	68.258	6.030
measurements	1.404	62.54	5.55/5.76

Comparison of all the values shows that the results obtained with 2D simulations must be taken with an extreme care. The 3D model revealed some effects which essentially influence the values of lumped parameters, but can not be taken into account with the idealized 2D approach. In all simulations the 3D model exhibits non-uniform field distribution in the transition from the pick-up to the leakage zone. This advantage of the 3D model predominates over the better accuracy of the finite element approximation (denser grid and higher order of approximating functions) of the 2D code.

We have shown that using different approaches to calculation of inductances gives similar, yet different results. Dispersion of the obtained values can be used as an estimate of the error and it seems to be more useful indicator, than the values of error shown by the numerical code.

Acknowledgements

This work has been partially supported by the European Union in the framework of European Social Fund through the Warsaw University of Technology Development Programme.

BIBLIOGRAPHY

- [1] W. Choromański, J. Kowara: PRT-Modeling and dynamic simulation of the track ant the vehicle, 13 International Conference of Automated People Movers, 23-26 May 2011, Paris - ASCE - American Society of Civil Engineers, Symposium Proceedings Book.
- [2] W. Choromański, G. Kamiński, B. Kamiński, J. Kowara: System Personal Rapid Transit - research, technology and development forecast for the XXI century, Polish-Chinese Seminar, ECO-Mobility - Innovative technologies, Conference materials, ISBN 978-83-60965-93-1;
- [3] Ferroxcube 3C90 Material specification, September 1, 2008, available at <http://ferroxcube.com>
- [4] N. Ida: Alternative approaches to the numerical calculation impedance, NDT International, Vol. 21, No. 1, pp. 27-35, 1988.
- [5] C. Harlander, R. Sabelka, S. Selberherr: A Comparative Study of Two Numerical Techniques for Inductance Calculation in Interconnect Structures, Simulation of Semiconductor Processes and Devices, pp. 254-257, Springer-Verlag, Wien 2001
- [6] Chang-Hwan Im, Hyun-Kyo Jung: Numerical computation of inductance of complex coil systems, International Journal of Applied Electromagnetics and Mechanics, Vol. 29, pp. 15-23, 2009
- [7] O.C. Zienkiewicz, J. Z. Zhu: A Simple Error Estimator and Adaptive Procedure for Practical Engineering Analysis, International Journal of Numerical Methods in Engineering, vol. 24, pp. 337-357, 1987.